

Proximity effect of vanadium on spin-density-wave magnetism in Cr films

E. Kravtsov*

Institut für Experimentalphysik/Festkörperphysik,

Ruhr-Universität Bochum,

D-44780 Bochum, Germany

and

Institute of Metal Physics,

620219 Ekaterinburg, Russia

A. Nefedov, F. Radu, A. Remhof, and H. Zabel

Institut für Experimentalphysik/Festkörperphysik,

Ruhr-Universität Bochum,

D-44780 Bochum, Germany

R. Brucas and B. Hjörvarsson

Department of Physics,

Uppsala University, Box 530,

S-75121 Uppsala, Sweden

A. Hoser

Institut für Kristallographie, RWTH-Aachen,

D-52056 Aachen, Germany

and

Institut für Festkörperforschung,

Forschungszentrum Jülich,

D-52425 Jülich, Germany

S. B. Wilkins
European Commission, JRC,
Institute for Transuranium Elements,
D-76125 Karlsruhe, Germany
and
European Synchrotron Radiation Facility,
F-38000 Grenoble, France

(Dated: May 26, 2020)

Abstract

The spin-density wave (SDW) state in thin chromium films is well known to be strongly affected by proximity effects from neighboring layers. To date the main attention has been given to effects arising from exchange interactions at interfaces. In the present work we report on combined neutron and synchrotron scattering studies of proximity effects in Cr/V films where the boundary condition is due to the hybridization of Cr with paramagnetic V at the interface. We find that the V/Cr interface has a strong and long-range effect on the polarization, period, and the Néel temperature of the SDW in rather thick Cr films. This unusually strong effect is unexpected and not predicted by theory.

*Electronic address: evgeny.kravtsov@ruhr-uni-bochum.de

I. INTRODUCTION

The spin density wave (SDW) magnetism in Cr has attracted much attention since its first discovery in 1958 [1, 2]. Its bulk behavior is well established and considerable progress has also been made towards understanding of the SDW magnetism in alloys with other transition metals (see reviews [3, 4, 5, 6] and references therein). During the last decade this field has regained much momentum because of a shift of the main focus towards thin Cr films and multilayers. The SDW behavior in these systems was found to display new features, differing drastically from the bulk ones due to dimensional and proximity effects.

Bulk Cr is an itinerant antiferromagnet displaying an incommensurate SDW (ISDW) below the Néel temperature $T_N=311$ K. The SDW consists of a sinusoidal modulation of the amplitude of the antiferromagnetically ordered magnetic moments. The SDW is a linear wave, propagating always along $\{100\}$ directions in the bcc Cr lattice, while the wave-vector is incommensurate with the Cr lattice periodicity. At the spin-flip transition temperature $T_{SF}=123$ K, the SDW polarization changes from longitudinal (LSDW) ($T \leq T_{SF}$, magnetic moments aligned parallel to the wave propagation direction) to transverse (TSDW) ($T \geq T_{SF}$, magnetic moments aligned perpendicular to the wave propagation direction). Elastic strains and chemical impurities in Cr may cause the SDW to become commensurate (CSDW). In some cases the CSDW phase may be stable at temperatures much higher than 311 K [3, 4]. Generally, in bulk Cr the SDW exists in a polydomain state below the Néel temperature, with magnetic domains populating all possible $\{100\}$ directions.

Investigations of the SDW in thin Cr films were initially motivated by the significant interest in exchange coupled Fe/Cr multilayers displaying a giant magnetoresistance effect [7]. Today, an extensive literature has evolved, which traces different aspects of the Cr magnetism in Fe/Cr systems [8, 9, 10, 11]. From these studies it was concluded that the formation of SDW magnetism in thin Cr films is governed by a strong exchange coupling acting at the Cr/Fe interface on the one hand and by the interface structure/disorder on the other hand [12, 13, 14]. Similar observations have also been made for the SDW behavior in other Cr/ferromagnet systems, such as Cr/Ni and Cr/Co [15].

Although a complete understanding of the SDW magnetism in Cr/ferromagnetic systems has not been reached yet, attention has, in part, shifted to layered heterostructures of Cr in contact with nonmagnetic metals. Among others, the SDW state in Cr/Ag [16], Cr/Cu[15],

and Cr/V [17, 18] has been investigated recently. In particular, the Cr/V system promises to provide new physics via the hybridization between very similar Fermi surfaces and the tunability of the Fermi surface with hydrogen uptake in the vanadium host lattice.

It is well known that the SDW behavior is connected with the peculiar features of the Cr Fermi surface providing nesting vectors between electron and hole sheets of similar shape [19]. Doping with V decreases the electron concentration, and, hence, the magnetic moment of Cr. This is opposite to doping with Mn atoms, which enhances the magnetic moment and drives Cr towards CSDW order [20]. Comprehensive investigations of bulk CrV alloys [21, 22, 23] have revealed a linear decrease of the Néel temperature with the V concentration, followed by a corresponding decrease in the SDW period. The effect was found to be so strong that a concentration of only 4 at. % V is enough to suppress totally the SDW state in Cr. The decrease of the Cr magnetic moment in dilute CrV alloys has recently been confirmed by Mössbauer spectroscopy studies with ^{119}Sn probe atoms [24].

From the above mentioned facts it is reasonable to expect a strong suppression of the Cr magnetic moment and the SDW near the Cr/V interface. Recent theoretical calculations of the Cr/V interface magnetic structure performed by different groups [25, 26, 27, 28, 29] confirm this notion. In addition, the calculations predict that the boundary V monolayer should gain an induced magnetic moment, similar to the Fe/V interface, where theoretical and experimental work established a small induced V moment, polarized opposite to the Fe moments [30, 31, 32, 33, 34]. The interface effects discussed so far are expected to be of short range and should damp out quickly at a distance of several monolayers from the interface. In Cr/V multilayers the damping effect should manifest itself by locating the node of the SDW in the vicinity of the Cr/V interfaces [35]. It should be noted, however, that all theoretical investigations assume that the interface is perfectly sharp and that the propagation of the SDW is in the direction normal to the interface. The propagation direction of the SDW is not a result of the various ab-initio calculations, but has been incorporated artificially.

Mibu et al. [17, 18] have recently provided experimental support for the outlined theoretical picture in a series of elegant experiments with Mössbauer spectroscopy by inserting the ^{119}Sn probe layers in Cr/V multilayers at different distances from the interfaces. They have given direct experimental evidence for a reduction of the Cr magnetic moment near the interface region. Cr was found nonmagnetic at distances up to 20 Å away from the interface, while at larger distances of about 40 Å the Cr magnetic moment increases again and reaches

values comparable to the bulk moment.

So far we have discussed the local and short range effects which occur close to the Cr/V interface. Next we draw our attention to the more global properties. For instance, it would be highly interesting to investigate whether the Cr/V proximity effect changes the Néel temperature and the SDW parameters, including period, polarization, and propagation direction. Some theoretical work points to these more global effects. According to Ref. [36, 37], surface effects in isolated Cr films may extend up to several thousands of Ångstroms. In a similar fashion the Cr/V interface may perturb the Cr SDW magnetism more extensively than assumed so far. This has to be verified by experiments.

In the present paper we address the above questions concerning the global perturbation of the Cr SDW magnetism by Cr/V interfaces and provide a systematic study of the SDW state in 2000 Å thick Cr(001) films grown on a 14 Å thick V(001) buffer layer. The Cr thickness is chosen to be large enough to ignore any local interface effects and to concentrate only on long-range effects arising from the Cr/V interface. The amount of V atoms in the V layer is comparable with a CrV alloy of corresponding V concentration. From neutron and synchrotron scattering experiments we establish the magnetic phase diagram of the system and reveal the Cr/V proximity effect on the SDW state in comparison to other Cr thin film systems, bulk Cr, and CrV alloys.

II. GROWTH AND SAMPLE CHARACTERIZATION

The sample was grown with a UHV magnetron sputtering system on a 20x20 mm² MgO(001) substrate. The deposition started with a V buffer layer of 14 Å thickness and continued with a 2000 Å thick Cr film. No protection layer was deposited, so a thin oxide layer is formed at the top of the Cr film [38]. During the deposition the substrate temperature was kept at 200°C. After the preparation the sample was cut into several parts to be used in different experiments. In particular, we used a 15x20 mm² sample for neutron measurements and a 5x5 mm² sample for x-ray experiments.

The structural information on the sample was obtained with x-ray diffraction studies done at the W1.1 and D3 beamlines of the HASYLAB, Germany. The measurements were performed at room temperature using a wavelength $\lambda = 1.5404$ Å. The in- and out-of-plane lattice parameters of the Cr film as well as the epitaxial relationship between the film and

MgO substrate were established precisely by analyzing the scattered intensity around the Cr (002) and (011) fundamental peaks. The epitaxial relation between Cr and MgO was confirmed to be Cr(001)[100]//MgO(001)[110] that is also valid for growth of Cr directly on the MgO(001) substrate without any buffer layer [39], which is equivalent with the well known 45° epitaxial relation observed for Fe(001) on MgO(001). The Cr lattice was found to have a slight tetragonal distortion determined by the difference between the out-of-plane lattice parameter $a^\perp = 2.8865 \pm 0.0005 \text{ \AA}$ and the in-plane lattice parameter $a^\parallel = 2.879 \pm 0.001 \text{ \AA}$.

Next we discuss the structural correlation length and the film mosaicity. In Fig. 1a is shown the radial x-ray scan through the Cr(002) reflection. The solid line represents a fit to the data points by using a single Gaussian line shape. The full width at half maximum (FWHM) is estimated to be $\Delta(2\theta) = 0.044^\circ$. According to the Scherrer equation

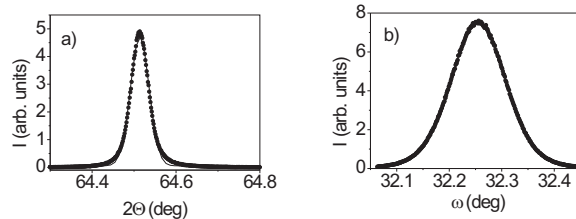


FIG. 1: a) Radial x-ray scan through the Cr(002) reflection. The solid line is a fit to the data points with a single Gaussian line shape. The width of the peak depends on the Cr film thickness and reflects a 100% structural coherence of the film; b) Transverse x-ray scan through the Cr(002) reflection. The solid line is a fit to the data points with a single Gaussian line shape with a FWHM of 0.10° .

[40], this FWHM value yields an out-of-plane structural coherence length of 2000 \AA , which corresponds exactly to the total Cr film thickness. In Fig. 1b is presented the transverse x-ray scan through the Cr(002) reflection. The solid line represents a fit to the data points by using a single Gaussian line shape. The FWHM is an estimate of the mosaic spread in the Cr film, which is about 0.10° . This is 5 times less than reported earlier for Cr growth on MgO(001) [39] and about 2 times less than Cr growth on a Nb(001) buffer layers [15]. Thus, the initial growth of a thin V buffer layer turns out to improve the Cr intralayer structure significantly.

III. SCATTERING EXPERIMENTS

When dealing with Cr thin film systems, one should distinguish between in-plane and out-of-plane SDW propagation directions and polarizations that are nonequivalent due to the broken symmetry at the interfaces. The Cr magnetic structure can be explored by elastic neutron scattering providing complete information on the SDW state. The magnetic moment modulation produces corresponding satellite reflections around forbidden bcc Bragg reflections, which can be detected with neutron scattering.

The SDW is accompanied by a charge density wave (CDW) and a strain wave (SW), corresponding to periodic modulations of the charge density and the lattice spacing, respectively. The modulation period of the SW and CDW is half the period of the SDW. The SW can be investigated via x-ray scattering, yielding information about the SDW period and propagation direction [41, 42, 43]. Although SW investigations do not reveal the SDW polarization, they have the advantage of a higher reciprocal space resolution, which is important for a precise determination of the SDW period. The application of neutron and X-ray scattering methods to the determination of the SDW parameters has been reviewed in some detail in a number of papers. We will not repeat this here and refer the interested reader to published papers and reviews for further information [3, 13, 15, 44].

A. Synchrotron scattering measurements

Synchrotron scattering experiments were performed at the ID20 magnetic scattering undulator beamline of the ESRF (Grenoble, France) [45, 46]. The incident photon beam delivered by two phase undulators was 99.8 % linearly σ -polarized in the sample plane. The primary slits in the optical system were set to utilize the first harmonic of the undulators. The incident beam energy was selected to be slightly below the Cr absorption edge of 5.989 keV by using a Si(111) double crystal monochromator. The polarization of the scattered beam was analyzed by using a pyrolytic graphite PG(004) analyzer to select pure $\sigma\sigma$ scattered intensity, also providing a drastic reduction of the background signal. The measurements were taken at temperatures between 15 and 300 K by using a displax cryostat equipped with Be windows.

To determine the propagation direction of the SW and SDW we first performed two

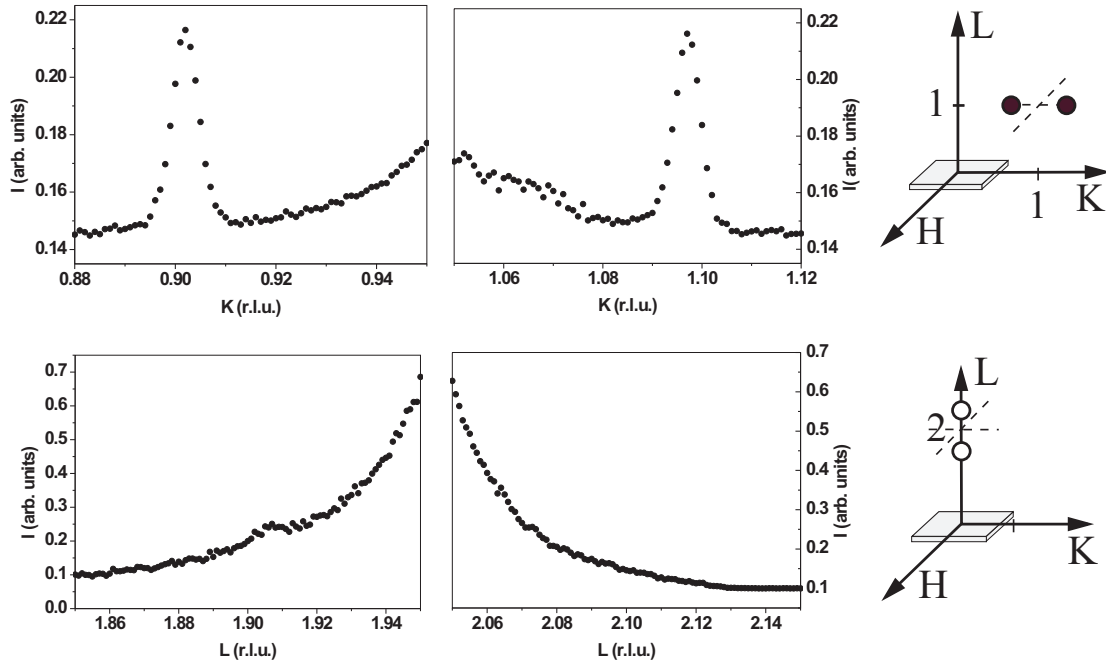


FIG. 2: Synchrotron radiation scans (a) along the K direction around the Cr(011) peak and (b) along the L direction around the Cr(002) reflection taken at 15K without polarization analysis. The fundamental (002) and (011) Cr peaks are removed from the figures since their intensity is many orders of magnitude higher than the intensity of the satellite reflections.

screening scans: one scan at the Cr(011) reflection in the K direction to check possible in-plane SW propagation, and one scan along the L direction, crossing the Cr(002) reflection to search for out-of-plane SW. In Fig. 2 are shown the above scans measured at 15K without polarization analysis. The fundamental (002) and (011) Cr peaks are removed from the figures for clarity as their intensity is many orders of magnitude higher than the intensity of the satellite reflections. In the panel on the right side the scan directions are indicated. The circles refer to satellite reflections allowed by the selection rules but not detected, whereas closed circles refer to allowed and detected satellites. From the recorded scans it is evident that in our case the strain wave propagates entirely in the film plane, whereas the out-of-plane wave is completely suppressed. In subsequent experiments we have analyzed in more detail the in-plane SW component. In Fig. 3 we show the satellites position and intensity measured for different temperatures in the range between 30 and 300 K. As evident from the picture, the satellites positions move smoothly towards the (011) peak as temperature

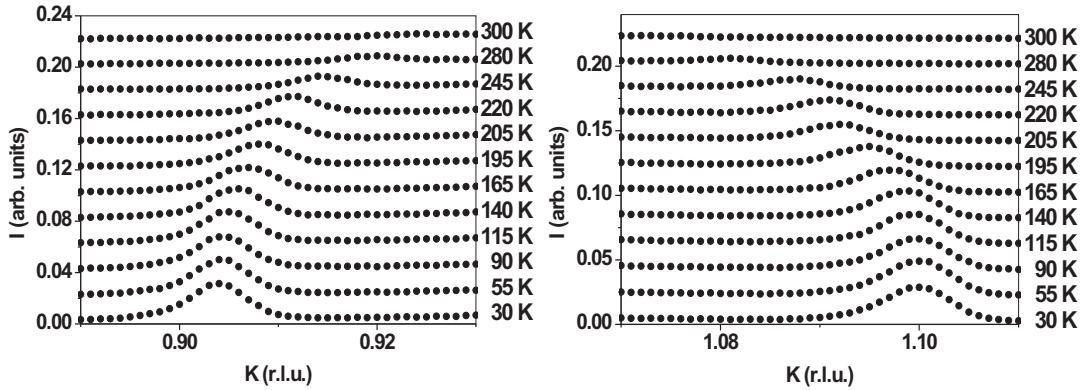


FIG. 3: Synchrotron measurement of the temperature dependence of the scattered intensity along K direction around the Cr(011) reflection taken with polarization analysis of the scattered beam. The fundamental Cr(011) peak is removed from the figure, the curves and the individual scans are shifted vertically by a constant factor for clarity.

increases, while the intensity decreases continuously with temperature. It is important to note that the FWHM of the satellite peaks, about 0.007 in r.l.u., is essentially independent of temperature over the entire temperature region investigated. At 300 K the satellite peak intensity has vanished, which can be taken as the Néel temperature of our system. The information on the SW behavior inferred from the synchrotron scattering data will be discussed further below together with the neutron scattering results.

B. Neutron scattering measurements

The neutron scattering experiments were performed on the triple-axis spectrometer UNIDAS installed at the FRJ-2 research reactor (Forschungszentrum Jülich, Germany). In the experiment we used the (002) reflection of a highly oriented PG double crystal monochromator to select a neutron beam wavelength of $\lambda = 2.351 \text{ \AA}$. Another PG analyzer and a system of special slits and collimators were used to improve the instrumental resolution by reducing the neutron beam divergence and the background radiation. For these experiments the spectrometer was operated as a diffractometer by fixing the analyzer crystal to zero energy transfer. In this mode the background radiation is effectively filtered out. The contamination of the $\lambda/2$ radiation was removed by placing a PG transmission filter in the

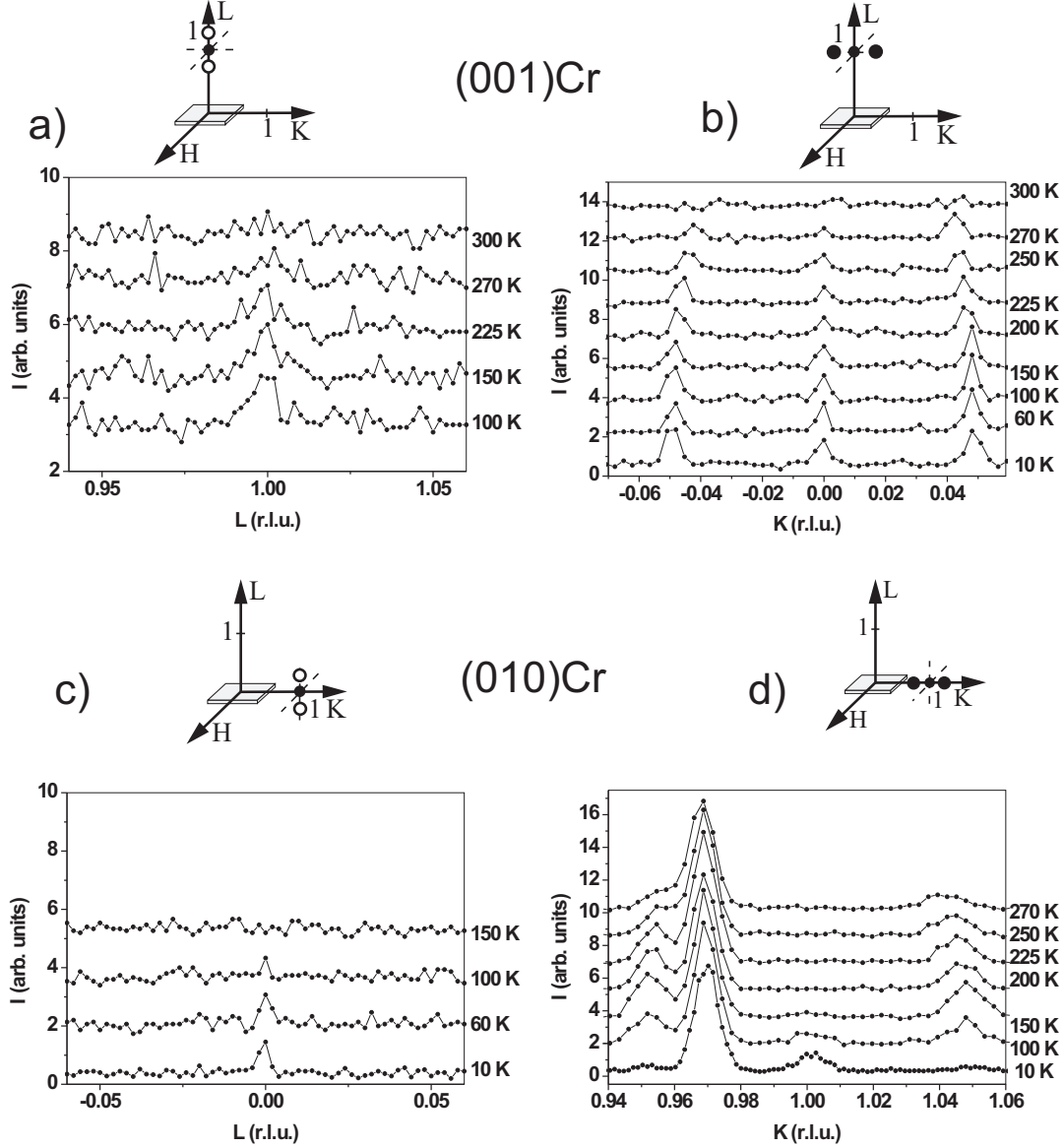


FIG. 4: Neutron scattering scans taken at the Cr(010) and the Cr(001) positions to explore the SDW polarization. The scans recorded at different temperatures are depicted with an offset in the vertical direction for clarity. The strong temperature-independent peak at $K \sim 0.97$ r.l.u. in Fig. 4d is due to the MgO(022) reflection for the $\lambda/2$ harmonics.

incident neutron beam. The measurements were taken at temperatures between 30 and 300 K by using a displex cryostat with Al windows.

In Fig. 4 are presented neutron diffraction scans performed in the vicinity of the Cr(010) and Cr(001) positions in the reciprocal space. Above each set the scan directions are in-

dedicated. Open circles refer to satellite reflections allowed by the selection rules but not detected, whereas closed circles refer to allowed and detected reflections. The above neutron results are sufficient for a complete analysis of the SDW parameters including their temperature dependence. We note that the neutron scattering results are in complete agreement with the synchrotron scattering results. As seen in Fig. 4, the satellite reflections due to the incommensurate SDWs occur only in the K direction in the vicinity of the (001) and (010) reflections. This implies that the SDW propagates in the film plane, as already conjectured from the x-ray scans. The Néel temperature is estimated to be about 300 K, which agrees with the synchrotron results. The temperature dependence of the SDW polarization is nearly identical to the one observed in bulk Cr [47]. At low temperatures we observe a longitudinal SDW. Above 100 K a spin-flip transition occurs to an in-plane transverse SDW. However, in contrast to the bulk behavior, the longitudinal and the transverse SDW are bi-domain, and in both cases the Cr magnetic moments are aligned parallel to the film plane.

In addition to the satellite reflections from ISDW phase, we also observe the (001) reflection corresponding to CSDW. The commensurate phase coexists with the incommensurate one at all temperatures up to the Néel temperature. From Fig. 4 we notice that the intensity of the (001) reflection decreases smoothly with increasing temperature up to 300 K, while the (010) peak intensity disappears above 150 K. Thus the polarization of the CSDW is similar to the ISDW: the magnetic moments remain in the film plane for all temperatures. Below 100 K the magnetic moments are oriented parallel to the H direction, and above 150 K parallel to the K direction. The transition from one to the other polarization direction occurs continuously between 100 K to 150 K. The integrated intensity of the CSDW reflection is about 10 % of that of the ICDW satellites. Both the CSDW and ISDW reflections have the same FWHM, which is directly connected with the in-plane SDW correlation length.

In Fig. 5 is depicted the temperature phase diagram for the V/Cr system. Both the ISDW and the CSDW propagate always in the film plane with the magnetic moments lying also in the film plane. The spin-flip transition for both phases starts at the same temperature of about 100 K. While the spin-flip transition for the ISDW is more or less sharp, the spin reorientation transition for the CSDW is spread over a wide temperature interval of about 50 K.

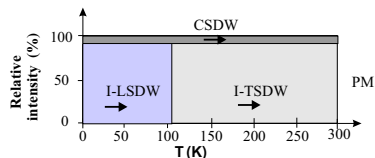


FIG. 5: Qualitative magnetic phase diagram for the spin density wave in a 2000 Å thick Cr(001) film deposited on a MgO(001) substrate with a 15 Å thick V buffer layer. The phase diagram is the result of combined synchrotron and neutron-scattering experiments, as described in the text.

IV. DISCUSSION

The synchrotron and neutron scattering results described in the previous section allow us to draw a clear picture of the SDW behavior within the Cr/V system. To work out the essential details arising from the Cr/V proximity effect, we will compare the results obtained with those known from reference systems: bulk Cr, dilute CrV alloy and single Cr films on other paramagnetic or ionic substrates.

First we discuss possible effects of the vanadium buffer layer on the SDW polarization and

propagation direction. It is generally recognized now that the SDW propagation direction in thin Cr films is governed by strain effects from substrate and buffer layer, whereas the SDW polarization is mainly due to proximity effects from neighboring layers. In case of a 4000 Å thick Cr(001) film on a Al₂O₃(1 $\bar{1}$ 02) substrate with a Nb(001) buffer layer a mixture of in-plane transverse and out-of-plane longitudinal ISDW has been observed below the Néel temperature, while for a 3000 Å thick Cr film an out-of-plane LSDW is observed at low temperature, which transforms to a out-of-plane TSDW at higher temperatures [48, 49]. In all cases the Cr surfaces was uncapped and therefore was covered with a roughly 20 Å thick Cr₂O₃ layer, which forms by natural oxidation [38]. For a single 4500 Å Cr film grown on the MgO(001) substrate without any buffer layer, Kunnen et al. [39] observed a mixture of CDSW and ISDW, which propagate in the film plane, while the spins are oriented in the direction normal to the film plane. Our recent data for a 2000 Å Cr film at MgO(001) substrate [50] are in line with the results [39]. We found that the SDW propagates in the film plane, it has longitudinal polarization at temperatures below 100 K and transversal with out-of-plane spins at temperatures from 100 to 270 K. At higher temperatures we observed the in-plane CSDW with out-of-plane spins. The propagation direction agrees with our observations, but not the spin direction. So we conclude that the proximity effect from thin V layer is responsible for the SDW polarization.

This unusually strong proximity effect is unexpected and it is difficult to give its adequate explanation. Based on present state-of-art in the field, we would only suggest that the underlying mechanism is connected with induced magnetic polarization at the V/Cr interface. As mentioned in the Introduction, at V/Fe and at V/Co interfaces an induced V moment polarized antiparallel to the ferromagnetic moments has been established [31, 32, 51]. It is possible that a similar polarization may also occur at the V/Cr interface. In this case, the V magnetic moments are aligned parallel to the interface and are exchange coupled indirectly with the Cr magnetic moments across a non-magnetic layer at the interface [17]. This might explain the difference in spin orientation for Cr on plain MgO (out-of-plane) and for Cr on MgO with a thin buffer layer (in-plane).

The actually observed SDW may not only depend on the electronic properties of the boundary layer, but also on the strain state and thickness of Cr. To the best of our knowledge, there is no theoretical prediction available as concerns the orientational effects caused by paramagnetic boundary layers. We note, however, that the effect of pinning the SDW

nodes near the Cr/V interfaces as predicted by Hirai [35] does not apply in our case, since the SDW propagates in the layer plane.

Next we consider proximity effects of vanadium on other SDW parameters, in particular, on the SDW period. Since the synchrotron data on the SW are more precise than the neutron data, we use those to estimate the period of the SDW as a function of temperature. The data are plotted in Fig.6 and compared to the SDW period in bulk Cr [43] and in a 2000 Å thick Cr film grown on a thick Nb buffer layer [48]. Since no data are available for thin CrV films, we compare our results with a bulk $\text{Cr}_{0.995}\text{V}_{0.005}$ alloy [52, 53, 54]. This corresponds roughly to the same composition as $\text{Cr}(2000 \text{ \AA})/\text{V}(14 \text{ \AA})$ when mixed, which would result in a 0.7 at % alloy. As can be seen from the figure, the temperature dependence

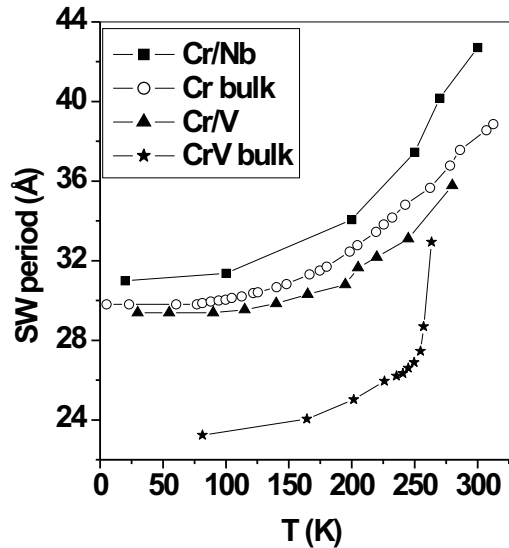


FIG. 6: Temperature dependence of the strain wave period in the Cr/V film and corresponding data for reference systems: 2000 Å Cr film on a thick Nb buffer layer [48], bulk Cr [43], and in bulk $\text{Cr}_{0.995}\text{V}_{0.005}$ alloy [52]. The solid lines connecting the data points are guides to the eye.

of the SW period in our Cr/V film is similar to that in other Cr thin film systems and in bulk Cr, but completely different from that in the $\text{Cr}_{0.995}\text{V}_{0.005}$ alloy. The value of the SW period in the Cr/V film is smaller than in bulk Cr and in other thin Cr films, but much larger than in the corresponding bulk CrV alloy. To our knowledge, the SW period observed in our Cr/V system is the smallest one observed so far in Cr-based thin films and multilayers.

In Fig. 7 we show the temperature dependence of the integrated intensity of the SW

satellite peaks for the same systems. The integrated intensity $I(t)$ is proportional to the square of the order parameter which, in turn, is proportional to the Cr magnetic moment. Its temperature dependence is a characteristic of the phase transition from the antiferromagnetic to the paramagnetic state in Cr. It is known that the temperature dependence $I(t)$ in bulk Cr can be described in analogy to the BCS theory of superconductivity [19].

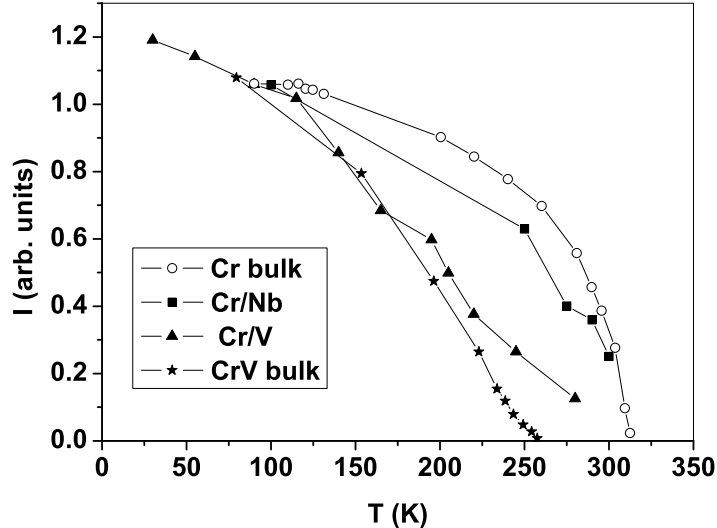


FIG. 7: Temperature dependence of the integrated intensity of the strain wave satellite reflections in the present Cr/V film and corresponding data for reference systems: 2000 Å Cr film at thick Nb buffer[48], bulk Cr [43], and integrated intensity of the spin density wave satellite reflections measured with neutron scattering in bulk CrV alloy with a V concentration of 0.5 at. % (from Noakes et al.[52]).

In the present Cr/V system we find a quasi-linear temperature dependence of $I(t)$ at low temperatures, which resembles the temperature dependence observed in CrV alloys [52], but which is drastically different from the $I(t)$ dependence seen in bulk Cr and other thin films. Noakes et al. [52] speculated that the unusual $I(t)$ behavior may not be an intrinsic feature of the CrV alloy, but due to strain effects. From our analysis it appears that the $I(t)$ dependence is an intrinsic property of the CrV systems. At higher temperatures the $I(t)$ for Cr/V deviates from that of the CrV alloy and stretches towards the bulk Néel temperature. Another important difference is the temperature dependence for the FWHM of the SW satellite peaks in Cr/V as compared to bulk Cr. According to Hill et al [43], in bulk Cr

the FWHM of the SW satellite reflection increases with temperature, implying a reduction of the SDW correlation length with increasing temperature. In Cr/V we find no change in the FWHM of the SW satellite peak over the entire temperature range and consequently no change in the correlation length.

V. CONCLUSIONS

We have studied the proximity effect of vanadium on the spin density wave magnetism in Cr/V films. The sample was grown with a UHV magnetron sputtering system on MgO(001) substrate with a 14 Å thick V(001) buffer layer. The Cr film exhibits a very high structural quality expressed by an out-of-plane coherence length corresponding to the film thickness and a very small mosaicity. The SDW properties were investigated by a combination of synchrotron scattering experiments to probe the strain waves and elastic neutron scattering to probe the spin density waves in the Cr film. It was shown that the V-Cr hybridization at the interface causes a strong and long-range influence on the SDW behavior in the Cr film. First, we found that the V-Cr interface hybridization changes the SDW polarization from out-of-plane to in-plane, i.e. the transverse incommensurate SDW propagates in the film plane and the magnetic moments are also in the plane. Second, for the SDW period and the order parameter we see a mixture of features which are typical for both, bulk CrV alloys and simple Cr films. The temperature dependence of the SDW period is similar to that in other Cr films but different from the one in CrV alloys. On the other hand, the value of the SDW period is smaller than in bulk Cr and other Cr films, which is a characteristic feature of CrV alloys. The Cr magnetic moment in Cr/V bilayers decreases quasi-linearly at low temperatures, which is also observed in some CrV alloys but not in bulk Cr or other Cr-based thin film systems. The Néel temperature corresponds to the bulk value. Above the Néel temperature for the incommensurate phase we do not observe any commensurate SDW, which we ascribe to the high quality of the film. In any case, the commensurate SDW plays only a minor role in the present Cr/V film system.

From the present experiments we conclude that the effect of a very thin V layer (14 Å) on a thick Cr film (2000 Å) is surprisingly large, changing drastically the global features of the SDW over the entire Cr film. This concerns the polarization of the SDW, the period, and the temperature dependence of the Cr magnetic moment at low temperatures. However, the

Néel temperature is roughly the same as in the bulk.

Acknowledgments

We would like to thank Dr. O. Seek and Dr. W. Morgenroth for help with the beamlines operation at the W1.1 and D3 instruments of the HASYLAB. This work has benefitted from collaborations within the Sonderforschungsbereich 491 'Magnetische Heteroschichten: Struktur und elektronischer Transport' funded by the Deutsche Forschungsgemeinschaft and from international collaborations supported by INTAS under project No. 01-0386. E.K. acknowledges support from RFBR.

-
- [1] L. Corliss, J.M. Hastings, and R.J. Weiss, Phys. Rev. Lett. **3**, 211 (1959).
- [2] V.N. Bykov, V.S. Golovkin, N.V. Agdeev, V.A. Ledvik, and S.I. Vinogradov, Dokl. Akad. Nauk SSSR **34**, 1149 (1958).
- [3] E. Fawcett, Rev. Mod. Phys. **60**, 209 (1988).
- [4] E. Fawcett, H.L. Alberts, V. Yu. Galkin, D.R. Noakes, J.V. Yakhmi, Rev. Mod. Phys. **66**, 25 (1994).
- [5] J.J.M. Franse, R. Gersdorf, Landolt-Börnstein, New Series III/19A, (New York:Springer-Verlag) 1986.
- [6] H.P.J. Wijn, Landolt-Börnstein, New Series III/32A, (New York:Springer-Verlag) 1997.
- [7] M.N. Baibich, J.M. Broto, A. Fert, F. Nguyen Van Dau, F. Petroff, P. Etienne, B. Greuzet, A. Friederich, and J. Chaselas, Phys. Rev. Lett. **61**, 2472 (1988).
- [8] J. Unguris, R. J. Celotta, and D.T. Pierce, Phys. Rev. Lett. **69**, 1125 (1992).
- [9] E.E. Fullerton, K.T. Riggs, C.H. Sowers, S.D. Bader, and A. Berger, Phys. Rev. Lett. **75**, 330 (1995).
- [10] A. Schreyer, J.F. Ankner, Th. Zeidler, H. Zabel, M. Schäfer, J.A. Wolf, P. Grünberg, and C.F. Majkrzak, Phys. Rev. B **52**, 16066 (1995); Europhys. Lett. **32**, 595 (1995).
- [11] P. Bödeker, A. Hucht, A. Schreyer, J. Borchers, F. Guthoff, H.Zabel, Phys. Rev. Lett. **81**, 914 (1998).
- [12] D. T. Pierce, J. Unguris, R.J. Celotta, M.D. Stiles, J. Magn. Magn. Matter. **200**, 290 (1999).
- [13] H. Zabel, J. Phys.: Condens. Matter **11**, 9303 (1999).
- [14] R. S. Fishman, J. Phys.: Condens. Matter **13**, R235 (2001).
- [15] P. Bödeker, A. Schreyer, H. Zabel, Phys. Rev. B **59**, 9408 (1999).
- [16] S. Demuynck, J. Meersschaut, J. Dekoster, B. Swinnen, R. Moons, A. Vantomme, S. Cottenier, and M. Rots, Phys. Rev. Lett. **81**, 2564 (1998).
- [17] M. Almokhtar, K. Mibu, A. Nakanishi, T. Kobayashi, T. Shinjo, J. Phys.: Condens. Matter **12**, 9247 (2000).
- [18] K. Mibu, M. Almokhtar, A. Nakanishi, T. Kobayashi, T. Shinjo, J. Magn. Magn. Matter. **226-230**, 1785 (2001).
- [19] A.W. Overhauser, Phys. Rev. **128**, 1437 (1962).

- [20] Eric E. Fullerton, J.L. Robertson, A.R. E. Prinsloo, H.L. Alberts, and S.D. Bader, Phys. Rev. Lett **91**, 237201 (2003).
- [21] Y. Hamaguchi, E.O. Wollan, W.C. Koehler, Phys. Rev. **138**, A737 (1965).
- [22] W.C. Koehler, R.M. Moon, A.L. Trego, A.R. Mackintosh, Phys. Rev. **151**, 405 (1966).
- [23] A.L. Trego, A.R. Mackintosh, Phys. Rev. **166**, 495 (1968).
- [24] S. M. Dubiel, J. Cieslak, E.E. Wagner, Phys. Rev. B **53**, 268 (1996).
- [25] A. Boussendel, A. Haroun, Thin Solid Films **325**, 201 (1998).
- [26] G. Bühlmayer, T. Asada, S. Blügel, Phys. Rev. B **62**, R11937 (2000).
- [27] B.A. Hamad, J.M. Khalifeh, Surf. Sci. **492**, 161 (2001).
- [28] A. Kellou, N.E. Fenineche, A. Tadjer, H. Aourag, Materials Chem. Phys. **80**, 215 (2003).
- [29] H. C. Herper, P. Weinberger, L. Szunyogh, and P. Entel, Phys. Rev. B **68**, 134421 (2003).
- [30] M.M. Schwickert, R. Coehoorn, M.A. Tomaz, E. Mayo, D. Lederman, W.L. O'Brien, Tao Lin, and G.R. Harp, Phys. Rev. B **57**, 13681 (1998).
- [31] A. Scherz, H. Wende, P. Pouloupoulos, J. Lindner, K. Baberschke, P. Blomquist, R. Wappling, F. Wilhelm and N. B. Brookes, Phys. Rev. B **64**, 180407 (2001).
- [32] A. Scherz, P. Pouloupoulos, R. Nünthel, J. Lindner, H. Wende, F. Wilhelm, and K. Baberschke, Phys. Rev. B **68**, 140401 (2003).
- [33] D. Laberge, K. Westerholt, H. Zabel, and B. Hjörvarsson, J. Magn. Magn Mater. **225**, 373 (2001).
- [34] V. Uzdin, K. Westerholt, H. Zabel, and B. Hjörvarsson, Phys. Rev. B **68**, 214407 (2003).
- [35] K. Hirai, Phys. Rev. B **66**, 132405 (2002).
- [36] S. M. Dubiel, J. Cieslak, Phys. Stat. Sol. (a) **191**, 577 (2002).
- [37] J. Cieslak, S. M. Dubiel, Phys. Stat. Sol. (a) **196**, 181 (2003).
- [38] A. Stierle, H. Zabel, Europhys. Lett. **32**, 365 (1997).
- [39] E. Kunnen, S. Mangin, V.V. Moshchalkov, Y. Bruynseraede, A. Vantomme, A. Hoser, K. Temst, Thin Solid Films **414**, 262 (2002).
- [40] B.E. Warren, X-ray Diffraction (New York: Dover Publications) 1990.
- [41] Y. Tsunoda, M. Mori, N. Kunotomi, Y. Teraoka, J. Kanamori, Solid State Commun. **14**, 287 (1974).
- [42] D. Gibbs, K.M. Mohanty, J. Bohr, Phys. Rev. B **37**, 562 (1988).
- [43] J.P. Hill, G. Helgesen, D. Gibbs, Phys. Rev. B **51**, 10336 (1995).

- [44] H. Zabel, A. Schreyer, P. Bödeker, and P. Sonntag *Spin density waves and proximity effects in thin epitaxial Cr films* in "Dynamical Properties of Unconventional Magnetic Systems", eds. A.T. Skjeltorp and D. Sherrington, NATO ASI Series E: Applied Sciences, Vol. 349, Kluwer Academic Publishers, Dordrecht/Boston/London, 1998.
- [45] A. Stunault, C. Vettier, F. de Bergevin, N. Bernhoeft, V. Fernandez, S. Langridge, E. Listrom, J.E. Lorenzo-Diaz, D. Wermeille, L. Chabert, R. Chagnon, *Synch. Rad.* **5**, 1010 (1998).
- [46] D. Mannix, P.C. de Camargo, C. Giles, A.J.A. de Oliveira, F. Yokaichiya, C. Vettier, *Eur. Phys. J. B* **20**, 19 (2001).
- [47] S.A. Werner, A. Arrott, H. Kendrick, *Phys. Rev.* **155**, 528 (1967).
- [48] P. Sonntag, P. Bödeker, A. Schreyer, H. Zabel, K. Hamacher, H. Kaiser, *J. Magn. Magn. Mater.* **183**, 5 (1998).
- [49] P. Sonntag, P. Bödeker, T. Thurston, H. Zabel, *Phys. Rev. B* **52**, 7363 (1995).
- [50] E. Kravtsov, R. Brucas, B. Hjörvarsson, G. McIntyre, A. Nefedov, F. Radu, A. Remhof, H. Zabel, unpublished.
- [51] Y. Huttel, G. van der Laan, T.K. Johal, N.D. Telling, and P. Bencok, *Phys. Rev. B* **68**, 174405 (2003).
- [52] D.R. Noakes, T.M. Holden, P.C. de Camargo, E. Fawcett, P. de V. DuPlessis, *J. Appl. Phys.* **64**, 5883 (1988).
- [53] P.C. de Camargo, A.J.A. de Oliveira, C. Giles, F. Yokaichiya, C. Vettier, *Mater. Sci. Forum* **302-303**, 33 (1999).
- [54] A.J.A. de Oliveira, O.F. de Lima, W.A. Ortiz, P.C. de Camargo, *Solid State Comm.* **96**, 383 (1995).